Chemical Physics Letters 511 (2011) 116–120

Contents lists available at ScienceDirect

Chemical Physics Letters

journal homepage: www.elsevier.com/locate/cplett

Formation of ZnO nanoparticles by laser ablation in neat water

Kuk Ki Kim [a], Daehyun Kim [b], Sang Kyu Kim [c], Seung Min Park [a], Jae Kyu Song [a,*]

[a] Department of Chemistry, Research Center for New Nano Bio Fusion Technology, Kyung Hee University, Seoul 130-701, Republic of Korea
[b] Yuseong High School, Daejeon 305-801, Republic of Korea
[c] Department of Chemistry, KAIST, Daejeon 305-701, Republic of Korea

ARTICLE INFO

Article history:
Received 13 April 2011
In final form 8 June 2011
Available online 12 June 2011

ABSTRACT

Zinc oxide (ZnO) nanoparticles were prepared in neat deionized water by laser ablation with various ablation times (10–40 min), fluences (50–130 mJ/pulse), and wavelengths (1064, 532, and 355 nm). The size and shape of the nanoparticles were affected only slightly by the ablation time and fluence at a wavelength of 1064 nm, which was explained by a dynamic formation mechanism with surface charge effects. The nanoparticles formed by ablation at 355 nm had a distinctive wire-shape with a small diameter, which was attributed to a continuous fragmentation and formation mechanism.

1. Introduction

Zinc oxide (ZnO) has attractive properties, such as a high luminescent efficiency, a wide band gap (3.36 eV), and a large exciton binding energy (60 meV), which has triggered extensive research on the properties of ZnO and the production of nanoparticles using physical and chemical methods [1–3]. Recently, laser ablation of a zinc metal target in liquid was reported to be an alternative for the production of ZnO nanoparticles [4–7]. Laser ablation in liquid has several advantages over traditional methods, such as technical simplicity and chemical pureness [8–10]. The most important advantage of this laser ablation method is that nanoparticles can be prepared with a native surface directly, which ensures several new benefits. However, growth control to limit the excessive coalescence of nanoparticles was often carried out with specific molecules, such as surfactant molecules, because nanoparticles prepared in neat water had a rather large size distribution [4–7]. Unfortunately, the introduction of surfactant molecules may lead to the loss of one of the main advantages of laser ablation in an aqueous solution because the surface of the nanoparticles is no longer nascent. Therefore, it is important to examine the laser ablation conditions that may lead to a narrow size distribution, even in neat water, which includes physical parameters, such as the ablation time, fluence, and wavelength. This Letter presents the experimental results on the formation of ZnO nanoparticles by laser ablation in neat water, which revealed the effects of the ablation times (10–40 min), fluences (50–130 mJ/pulse), and wavelengths (1064, 532, and 355 nm) on nanoparticle size and shape.

2. Experiment

The synthetic method of forming ZnO nanoparticles in neat water is described elsewhere [4]. ZnO nanoparticles were produced by the laser ablation of a zinc target (99.99%) placed in a Pyrex cell filled with deionized water. The zinc target was irradiated vertically by a Q-switched Nd:YAG laser (Surelite III) operating at 10 Hz, while the cell was rotated continuously to minimize the target aging effect and ensure a fresh surface of the zinc target in addition to a stirring effect during the formation of nanoparticles. The laser beam was focused to a beam diameter of 0.5 mm. The absorbance of the prepared solution was examined using a spectrophotometer (Shimadzu UV-1800). The photoluminescence (PL) in the solution was measured using a He–Cd laser (325 nm) as an excitation source. Transmission electron microscopy (TEM, Tecnai G2 F30) was used to observe the shape and size of the nanoparticles. The crystal structure of the nanoparticles in the dried film was examined by X-ray diffraction (XRD, Rigaku DMAX-IIIA) using the Cu Kα line, but crystalline peaks were barely observed in the prepared nanoparticles.

3. Results and discussion

3.1. Ablation time dependence of ZnO nanoparticles

Figure 1a shows the optical absorption spectra of the colloidal suspensions prepared in deionized water as a function of the ablation time by the fundamental output of the Nd:YAG laser (1064 nm) at a fluence of 100 mJ/pulse. The optical band gap of the nanoparticles was estimated from an extrapolation of a plot of $(\alpha h\nu)^2$ as a function of the photon energy in the absorption spectra. This is possible because the absorption coefficient (α) can be expressed as $\alpha h\nu \propto (h\nu - E_g)^{1/2}$ and the intercept provides a good

* Corresponding author. Fax: +82 2 966 3701.
E-mail address: jaeksong@khu.ac.kr (J.K. Song).

0009-2614/$ - see front matter © 2011 Elsevier B.V. All rights reserved.
doi:10.1016/j.cplett.2011.06.017

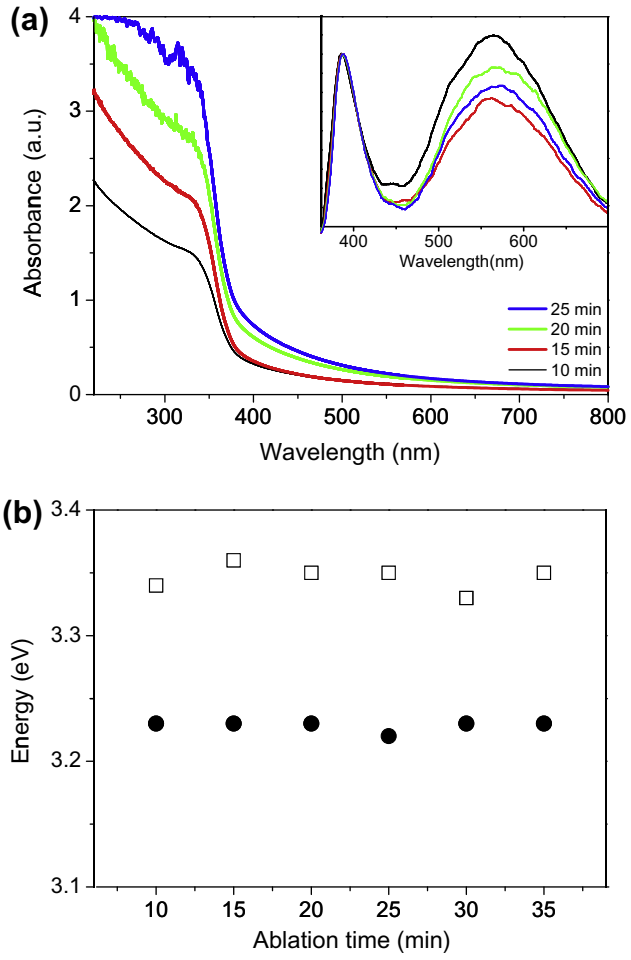

Figure 1. (a) Optical absorption spectra of ZnO nanoparticles prepared in deionized water as a function of the ablation time at 1064 nm with a fluence of 100 mJ/pulse. From the bottom to top, the absorption spectra are shown with increasing ablation time. The inset shows the PL spectra of the ZnO nanoparticles. The intensities are normalized for better comparison. (b) The optical band gaps (□) and exciton emission energies (●) of the ZnO nanoparticles as a function of the ablation time.

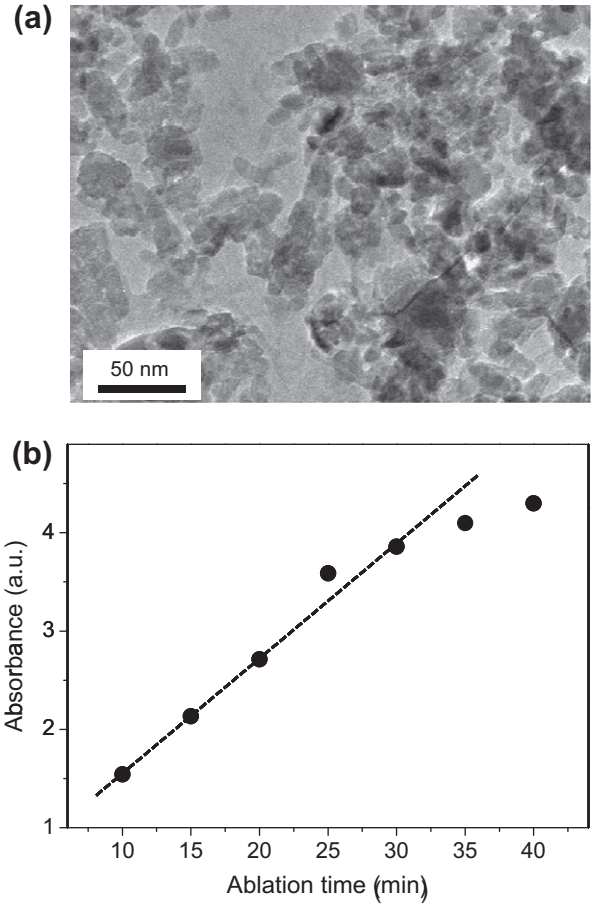

Figure 2. (a) Transmission electron microscopy (TEM) image of the ZnO nanoparticles prepared in deionized water at a fluence of 100 mJ/pulse and an ablation time of 20 min. (b) The absorbance at 320 nm in the optical absorption spectra as a function of the ablation time at 1064 nm with a fluence of 100 mJ/pulse. The absorbance of the ZnO nanoparticles increased almost linearly with the ablation time, but a saturation tendency was observed above 30 min.

approximation of the band gap (E_g) [11,12]. The band gap of the nanoparticles was ~3.35 eV, which agreed well with the band gap of ZnO. The band gaps did not exhibit a meaningful dependence on the ablation time, as shown in Figure 1b. The PL spectra in the inset of Figure 1a show that the emission peaks of all nanoparticles occurred at 384 nm, which was attributed to the exciton emission of ZnO [1–3,13]. Therefore, the main colloids prepared in the deionized water were concluded to be ZnO nanoparticles. Almost identical band gaps and exciton emission wavelengths irrespective of the ablation time indicated that the sizes of the ZnO nanoparticles were barely affected by the ablation time. In addition, the band gap of the nanoparticles was similar to that of the bulk materials [1–3], which suggested that quantum confinement effects were not significant. Indeed, the TEM image in Figure 2a shows that the mean diameter of the ZnO nanoparticles was ~20 nm, which was larger than the dimensions of an exciton Bohr radius (1.4–2.3 nm) [14,15], even though the size distribution was not narrow.

Nanoparticle formation in a surfactant solution by laser ablation has been explained using a dynamic formation mechanism [8–10]. The interaction of pulsed laser irradiation with the zinc target could create a plasma plume above the target surface, which consisted of zinc species, such as atoms and clusters. The plasma expanded adiabatically and created a shock wave at the interfaces, which increased the pressure and temperature of the plasma. At local high pressures and temperatures, the electrically excited and highly reactive zinc species were oxidized by water, which grew and coagulated rapidly in the plume. The formed clusters, which served as nuclei, induced further growth of nanoparticles. After extinction of the plume, which was maintained by the laser irradiation, the size of particles was increased rather slowly by the diffusive supplies of Zn/ZnO until the surfaces of the nanoparticles were covered with sufficient surfactant molecules. However, the nanoparticles formed in neat water could grow further by coagulation and coalescence in the absence of the surfactant molecules, which normally resulted in larger nanoparticle sizes in neat water than in solutions containing the surfactants [6,8,9]. In addition, the nanoparticles prepared in neat water could be polycrystalline or almost amorphous due to the strong coagulation and coalescence effects [16], which might explain why XRD did not reveal a crystalline structure of the ZnO nanoparticles formed in our study. It is noted that the nanoparticles were resistant to coalescence to some extent, which resulted in a mean diameter of ~20 nm. Since the ZnO nanoparticles were charged positively by insufficient oxidation in the aqueous solutions [6,17], the charged surfaces were suggested to be the main factor in overcoming the attractive van der Waals interactions between the nanoparticles [17]. Therefore, the similar nanoparticle sizes could be explained by the role of

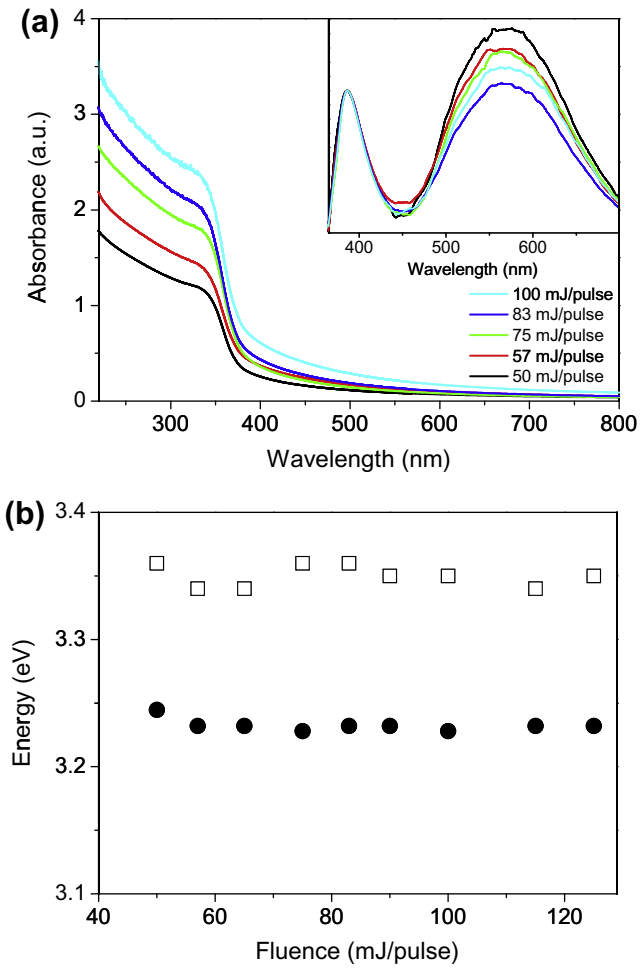

Figure 3. (a) Optical absorption spectra of ZnO nanoparticles prepared in deionized water as a function of the fluence at 1064 nm with an ablation time of 20 min. From the bottom to top, the absorption spectra are shown with increasing fluence. The inset shows the PL spectra of ZnO nanoparticles. The intensities are normalized for comparison. (b) The band gaps (□) and the exciton emission energies (●) of ZnO nanoparticles as a function of the fluence.

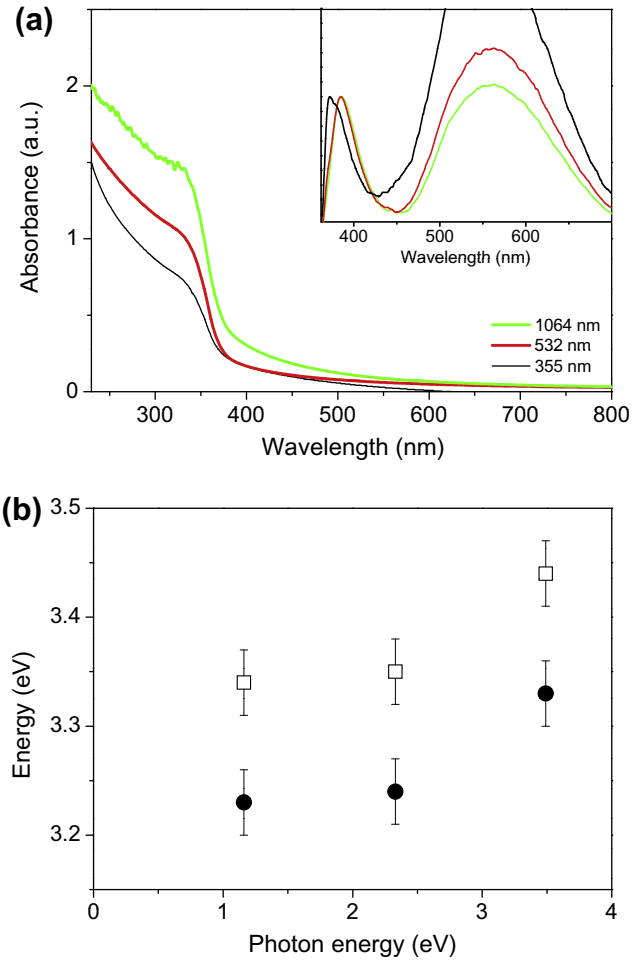

Figure 4. (a) Optical absorption spectra of the ZnO nanoparticles prepared in deionized water as a function of the ablation wavelength at a fluence of 100 mJ/pulse and an ablation time of 20 min. From the bottom to top, the absorption spectra are shown with increasing wavelength. The inset shows the PL spectra of the ZnO nanoparticles. The intensities are normalized for comparison. (b) The band gaps (□) and exciton emission energies (●) of the ZnO nanoparticles as a function of the ablation photon energy.

the surface charges because the surface charges responsible for size determination would not be related to the ablation time.

The absorbance of ZnO nanoparticles in neat water increased almost linearly with the ablation time of the target plate in the short time regimes (Figure 2b). Since the sizes of the ZnO nanoparticles were independent of the ablation time, the change in absorbance indicated that the number density of the nanoparticles increased with ablation time. However, the saturation tendency of the absorbance was observed in ablation times of 30 min and above, which implied a decrease in the ablation efficiency of the zinc species [9]. The surface properties of the zinc target plate may be altered by continuous ablation and the nanoparticles formed in the solution may screen the target plate by their own extinction, which reduced the ejection efficiency at a long ablation times.

The visible emission centered at 560 nm comes from the well-known defects of oxygen vacancies [18,19], which could possibly be attributed to insufficient oxidation in the aqueous solutions [6,17]. Since visible emission is related mainly to the surface states in ZnO [18,19], the surface areas of the nanoparticles might be important. Therefore, the intensities of the visible emission were not related to the ablation time (inset of Figure 1b) because the sizes and concomitant surface areas were affected only slightly by ablation time. However, the non-identical intensities of visible emission despite the similar surface areas remain to be elucidated in further studies.

3.2. Fluence dependence of ZnO nanoparticles

To understand fluence effects on nanoparticle formation, the nanoparticles were prepared in deionized water as a function of the fluence at 1064 nm with an ablation time of 20 min. The band gaps of the ZnO nanoparticles estimated from the optical absorption spectra (Figure 3a) were not dependent on the fluence of 1064 nm, as shown in Figure 3b. In addition, the PL spectra in the inset of Figure 3a also show that the exciton emission of the nanoparticles was similar, suggesting that the nanoparticle sizes were comparable, as observed in the dependence on the ablation time. Since the plume size of the zinc species was related to the fluence [9,20,21], the nanoparticle in the dynamic formation mechanism could be affected by the fluence. Indeed, the absorbance (number density) of the nanoparticles increased with increasing fluence (Figure 3a). But the nanoparticle sizes were controlled only slightly by the fluence because the sizes were determined mainly by the surface charges. Therefore, the fluence changed the densities of the nanoparticles in neat water, but

could not control the surface charges and concomitant sizes of the nanoparticles.

3.3. Wavelength dependence of ZnO nanoparticles

To find which parameters controlled size, the nanoparticles were prepared in deionized water at different ablation wavelengths, such as 1064, 532, and 355 nm, at the same fluence of 100 mJ/pulse and ablation time of 20 min. Figure 4a shows the optical absorption spectra of the ZnO nanoparticles. The band gap of the nanoparticles formed by 355 nm (Z355) was larger than those formed by 1064 nm (Z1064) and 532 nm (Z532), as shown in Figure 4b. The PL spectra in the inset of Figure 4a indicated that the exciton emission of Z355 (372 nm) was also blue-shifted from those of Z1064 and Z532 (384 nm). In addition, a difference was observed in the TEM images (Figure 5), which revealed that a wire-shape of Z355 with a mean diameter of ~4 nm was distinct from the spherical shapes of Z1064 and Z532 with mean diameters of ~20 nm. Therefore, the increase in the band gap and the blue-shift of the exciton emission (~0.1 eV) were attributed to quantum confinement effects.

When the dimension of a ZnO nanoparticle is comparable to the Bohr radius of an exciton, the band gap changes with the size of the spherical nanoparticles [22]:

$$\Delta E_g(R) = \frac{\pi^2\hbar^2}{2R^2}\left(\frac{1}{m_e^*}+\frac{1}{m_h^*}\right) \quad (1)$$

where $E_g(R)$ is the band gap shift in the spherical nanoparticle with a radius of R, m_e^* is the effective mass of the electron, and m_h^* is the effective mass of the hole. The band gap shift of a spherical nanoparticle with a diameter of 4.0 nm was calculated to be 0.27 eV. The difference between the experimental (0.1 eV) and estimated band gap shift (0.27 eV) was attributed to the fact that Z355 was not spherical. Indeed, the band gap of the nanowires was also affected by their length, even though the dependence on length was not as sensitive as the dependence on the diameter [23,24]. A wire-shaped nanoparticle with a diameter of 2.2 nm (an effective diameter of 2.6 nm) and a length of 43 nm showed a band gap shift of 0.23 eV [25], suggesting that the band gap shift at a diameter of 4.0 nm was in the range of 0.07–0.10 eV. This range matched the observed band gap shift, which supported that quantum confinement effects were responsible for the increase in the band gap of Z355. However, the difference in the band gap and exciton emission wavelength between Z1064 and Z532 was not clearly distinguishable. The similar mean diameters and broad size distributions might explain the small difference between Z1064 and Z532. In addition, their dimensions being beyond the quantum confinement regime were also partially responsible.

The wire-shape with a small diameter was observed only in Z355, which was related to the photon energy of 355 nm beam being larger than the band gap. The photofragmentation of the nanoparticles could have occurred due to band gap absorption at 355 nm during nanoparticle formation. Even after growth, the nanoparticles were exposed to subsequent irradiation at a repetition rate of 10 Hz, leading to continuous 'fragmentation and formation' of the nanoparticles during the entire ablation period [26]. It is noted that spherical ZnO nanoparticles were formed in neat water by ablation at 355 nm [6]. The vital difference was the fluence at 355 nm, which was responsible for photofragmentation, because the wire-shape was formed by a beam with the 4-fold higher fluence than that reported for the spherical shaped nanoparticles. In addition, when the zinc target plate was absent the size of the nanoparticles was reduced almost isotropically by photofragmentation due to band gap absorption of ZnO [4]. Therefore, the wire-shape was related to the directional growth of ZnO along the *c*-axis with a wurtzite structure [1–3], although the fragmentation took place approximately isotropically. In this regard,

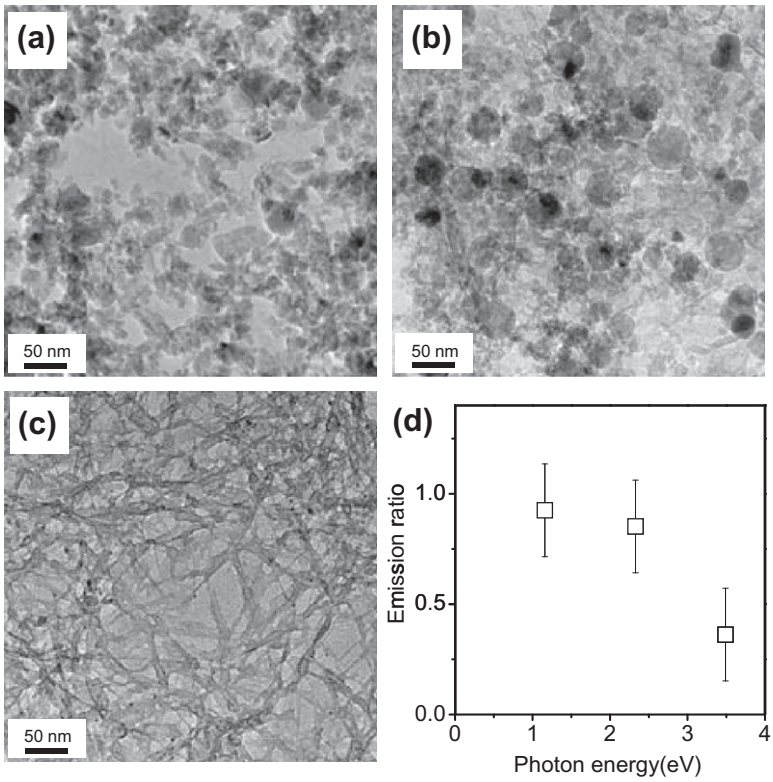

Figure 5. The TEM images of ZnO nanoparticles prepared in deionized water (a) at 1064 nm (Z1064) (b) at 532 nm (Z532) (c) at 355 nm (Z355) with a fluence of 100 mJ/pulse and an ablation time of 20 min. (d) The exciton to defect emission (exciton/defect) intensity ratio as a function of the ablation photon energy.

the wire-shape of Z355 could be formed by the accumulated effect of continuous fragmentation and formation, despite a more or less random coagulation and coalescence in neat water [6]. However, Z1064 and Z532 were spherical due to random coagulation and coalescence without the photofragmentation effect, since the band gap absorption of ZnO was not present in the irradiation at 1064 and 532 nm. We note that the absorption and emission spectra of Z532 were not identical to those of Z1064, despite a similar formation mechanism. Presumably, the ablation propensity of the zinc species might vary based on the fact that the number of the high-energy photons (532 nm) was a half that of the low-energy photons (1064 nm) at the same fluence of 100 mJ/pulse.

The strong visible emission of Z355 in Figure 4a was explained by the small diameter because defect emission was dependent on the surface states of the ZnO. In small nanoparticles, such as Z355, the surface to volume ratio is high, which led to a large surface area and a concomitant high defect density. Therefore, the defect emission of Z355 was stronger than those of Z1064 and Z532, as observed in the exciton to defect emission intensity ratio (Figure 5d).

4. Summary

ZnO nanoparticles prepared in deionized water showed a similar band gap and exciton emission wavelength irrespective of the ablation time and fluence at 1064 nm, which indicated that the size of the ZnO nanoparticles was affected only slightly by the ablation time and fluence. In the absence of surfactant molecules, nanoparticle formation was controlled mainly by the surface charges related to the insufficient oxidation in aqueous solution. However, the ablation time and fluence had a significant effect on the density of the ZnO nanoparticles. The band gap and exciton emission wavelength of Z355 were different from those of Z1064 and Z532, which was attributed to quantum confinement effects, as supported by the TEM images. The wire-shape of Z355 suggested a non-negligible photofragmentation of the nanoparticles mainly due to the photon energy at 355 nm.

Acknowledgements

This research was supported by Basic Science Research Program through the National Research Foundation of Korea (NRF) funded by the Ministry of Education, Science and Technology (NRF-2009-0 068 705). This work was also supported by the National Research Foundation of Korea Grant funded by the Korean Government (MEST, NRF-2009-C1AAA001-0 092 939).

References

[1] M.H. Huang et al., Science 292 (2001) 1897.
[2] J. Joo, S.G. Kwon, J.H. Yu, T. Hyeon, Adv. Mater. 17 (2005) 1873.
[3] C. Klingshirn, Phys. Stat. Sol. (b) 9 (2007) 3027.
[4] J.J. Moon, J.K. Song, S.M. Park, Bull. Kor. Chem. Soc. 30 (2009) 1616.
[5] K.Y. Niu, J. Yang, S.A. Kulinich, J. Sun, X.W. Du, Langmuir 26 (2010) 16652.
[6] H. Usui, Y. Shimizu, T. Sasaki, N. Koshizaki, J. Phys. Chem. B 109 (2005) 120.
[7] Z. Yan, R. Bao, D.B. Chrisey, Chem. Phys. Lett. 497 (2010) 205.
[8] F. Mafuné, J.-Y. Kohno, Y. Takeda, T. Kondow, J. Phys. Chem. B 104 (2000) 8333.
[9] F. Mafuné, J.-Y. Kohno, Y. Takeda, T. Kondow, J. Phys. Chem. B 107 (2003) 4218.
[10] C. Liang, Y. Shimizu, N. Koshizaki, J. Phys. Chem. B 107 (2003) 9220.
[11] Y.S. Wang, P. Thomas, P. Brien, J. Phys. Chem. B 110 (2006) 21412.
[12] N.G. Semaltianos, S. Logothetidis, N. Frangis, I. Tsiaoussis, W. Perrie, G. Dearden, K.G. Watkins, Chem. Phys. Lett. 496 (2010) 113.
[13] S.Y. Kim, Y.S. Yeon, S.M. Park, J.H. Kim, J.K. Song, Chem. Phys. Lett. 462 (2008) 100.
[14] B. Gil, A.V. Kavokin, Appl. Phys. Lett. 81 (2002) 748.
[15] R.T. Senger, K.K. Bajaj, Phys. Rev. B 68 (2003) 45313.
[16] S.Z. Khan et al., J. Nanopart. Res. 11 (2009) 1421.
[17] C. He, T. Sasaki, H. Usui, Y. Shimizu, N. Koshizaki, J. Photochem. Photobiol. A 191 (2007) 66.
[18] M.L. Kahn, T. Cardinal, B. Bousquet, M. Monge, V. Jubera, B. Chaudret, Chem. Phys. Chem. 7 (2006) 2392.
[19] H. Zeng, G. Duan, Y. Li, S. Yang, X. Xu, W. Cai, Adv. Funct. Mater. 20 (2010) 561.
[20] A.V. Kabashin, M. Meunier, J. Appl. Phys. 94 (2003) 7941.
[21] S.Z. Khan, Z. Liu, L. Li, Appl. Phys. A 101 (2010) 781.
[22] L.E. Brus, J. Chem. Phys. 80 (1984) 4403.
[23] J. Hu, L.-W. Wang, L.-S. Li, W. Yang, A.P. Alivisatos, J. Phys. Chem. B 106 (2002) 2447.
[24] D. Katz, T. Wizansky, O. Millo, E. Rothenberg, T. Mokari, U. Banin, Phys. Rev. Lett. 89 (2002) 086801.
[25] Y. Gu, I.L. Kuskovsky, M. Yin, S. O'Brien, G.F. Neumark, Appl. Phys. Lett. 85 (2004) 3833.
[26] N. Matsuo, H. Muto, K. Miyajima, F. Mafuné, Phys. Chem. Chem. Phys. 9 (2007) 6027.